UDC 621.314 https://doi.org/10.20998/2074-272X.2026.1.09

N. Guettaf, S.E.I. Guettaf, T. Zeghloul, H. Nouri

Numerical study of particles trajectories in a multifunctional electrostatic separator powered by photovoltaic system

Introduction. *Electrostatic separation is a growing technology in the recycling industry. It is an effective technology for processing plastics and metallic materials in the form of granular mixtures or fine powders from waste electrical and electronic equipment.* ***Problem.*** *Understanding the various physical phenomena occurring in the separation zone is crucial for improving the efficiency of electrostatic separation devices. This has led to the adoption of efficient and reliable numerical models for simulating particle trajectories. The* ***goal*** *of the work is to represent graphically the trajectories of two insulating charged polypropylene particles of different sizes (2 mm and 4 mm) in the multifunctional electrostatic separator powered by photovoltaic (PV) system use a multipoint electrodes as charging device employing numerical simulation and demonstrate its effectiveness and reliability for the study of particles trajectories by integrating PV panels as a power source for electrostatic separators according to the recommendations of the new energy system.* ***Methodology.*** *Using the Euler-Cromer method as numerical model to solve the equation of motion of the particles. This method was based on the calculation of the electric field intensity, which is done by the COMSOL Multiphysics software, which uses the finite element method (FEM). The numerical simulation was carried out using MATLAB software by varying the voltage applied to the active electrodes of the multifunctional electrostatic separator suggested, and the distance between them, taking into account the influence of electrostatic and mechanical forces on the charged insulating particles as they pass through the separation zone. The* ***results*** *were showed that the numerical model used is an effective and reliable tool for the study of particles trajectories.* ***Scientific novelty*** *of this work is to integrate PV panels as the main low-voltage energy source at the input of the high-voltage generator supplying the electrostatic separator with an optimal voltage of 30 kV. In addition, this numerical study has used electrostatic forces, gravitational forces, and dynamic forces simultaneously.* ***Practical value.*** *The numerical simulation was contributed to a thorough understanding of various physical phenomena occurring in the separation zone and was considered a tool to validate experimental results.* References 31, tables 2, figures 14.

Key words: **electrostatic separation, electric field, photovoltaic system, numerical modeling, particle trajectories, waste electrical and electronic equipment.**

Вступ. *Електростатична сепарація є технологією, що розвивається в індустрії переробки. Це ефективна технологія для переробки пластику та металевих матеріалів у вигляді гранульованих сумішей або тонких порошків із відходів електричного та електронного обладнання.* ***Проблема***. *Розуміння різних фізичних явищ, що протікають у зоні поділу, має вирішальне значення для підвищення ефективності пристроїв електростатичної сепарації. Це призвело до прийняття ефективних та надійних чисельних моделей для моделювання траєкторій частинок.* ***Мета*** *статті полягає у графічному представленні траєкторії двох ізолюючих заряджених частинок поліпропілену різних розмірів (2 мм і 4 мм) в багатофункціональному електростатичному сепараторі, що працює від фотоелектричної (PV) системи, використовуючи багатоточкові електроди як зарядний пристрій, застосовуючи чисельне моделювання та демонструючи ефективність PV панелей як джерела живлення для електростатичних сепараторів відповідно до рекомендацій нової енергетичної системи.* ***Методика***. *Використання методу Ейлера-Кромера як чисельної моделі для вирішення рівняння руху частинок. Даний метод заснований на розрахунку напруженості електричного поля, яке виконується за допомогою програмного забезпечення COMSOL Multiphysics, що використовує метод скінченних елементів (FEM). Чисельне моделювання проводилося з використанням програмного забезпечення MATLAB шляхом зміни напруги, що подається на активні електроди пропонованого багатофункціонального електростатичного сепаратора, та відстані між ними з урахуванням впливу електростатичних та механічних сил на заряджені частинки ізолюючі при їх проходженні через зону поділу.* ***Результати*** *показали, що використана чисельна модель є ефективним і надійним інструментом для дослідження траєкторій частинок.* ***Наукова новизна*** *роботи полягає в інтеграції PV панелей як основного джерела енергії низької напруги на вході високовольтного генератора, що живить електростатичний сепаратор оптимальною напругою 30 кВ. Крім того, в даному чисельному дослідженні одночасно використовувалися електростатичні, гравітаційні та динамічні сили.* ***Практична значимість***. *Чисельне моделювання сприяло глибокому розумінню різних фізичних явищ, що відбуваються в зоні поділу, та розглядалося як інструмент для підтвердження експериментальних результатів.* Бібл. 31, табл. 2, рис. 14.

Ключові слова: **електростатична сепарація, електричне поле, фотоелектрична система, чисельне моделювання, траєкторії частинок, відходи електричного та електронного обладнання.**

Introduction. During recent years, the world has been experiencing a rapid pace of consumption of electrical and electronic devices for domestic and industrial use. This pace is due to two main factors: the remarkable technical advances that have affected most modern devices. The digital and electronic transformation has brought about a radical change in the lives, businesses, relationships, and affairs of individuals and society [1, 2]. At the end of 2022, waste electrical and electronic equipment (WEEE) was estimated at around 62 million tones, or an average of 7.8 kg per capita, of which 22.3 % (13.8 million tones) was destined for proper collection and recycling [3]. This category of waste has caused numerous economic, social, and environmental crises. It also occupies vast areas, which is a source of concern for human health and a major challenge for sustainable development [4].

Over the past 20 years, the recycling industry has emerged as a new resource for genuine environmental restructuring and has been embraced as a main solution in the WEEE recycling [4, 5]. Electrostatic separation is an efficient technique that is built into the new energy paradigm. In addition to the electrostatic separation, there are several other electrical separation methods used across industries like electrophoresis, electro pulse, dielectrophoresis, conductivity-based separation, and magneto-electrostatic hybrid separation. It stands out for its minimal energy consumption, low operating and maintenance costs, and environmental friendliness, but has drawbacks in the sensitivity of humidity and particle surface conditions [6–8]. It is also highly efficient compared to the other methods mentioned, and a feasible transformation technology for plastics, and metallic materials from WEEE, such as electric cables, and electronic cards [9], as well as in agricultural food [10], and mining products [11]. The WEEE recycling process

goes through 4 original stages, which are as follows. First, plastics and metals from WEEE are sorted according to their type. Second, they are cut into millimeter granular mixtures of sizes ranging from 1 to 6 mm or ground into fine powders of sizes less than 1 mm, having the same density and electrical conductivity [12–14]. Third, the granular mixtures or fine powders are charged by at least one or more electrical charging mechanisms such as corona discharge, electrostatic induction, and triboelectric effect. Finally, the granular or powdery mixtures are separated in an intense electric field generated by two electrodes coupled to a high-voltage DC power source of opposing polarity [4].

Currently, there are many efficient and reliable electrostatic separators that have been applied to sort the components of granular mixtures or fine powders. These include drum electrostatic separators [15], vertical electrode electrostatic separators [16], tribo-aero-electrostatic separators with conveyor belts [17], tribo-aero-electrostatic separators with two rotating disks [18], free-fall electrostatic separators [19], and multifunctional electrostatic separators of the metal belt conveyor type [20].

The multifunctional electrostatic separator and the free-fall electrostatic separator are two of the most favored and useful models for sorting the parts of electrical and electronic equipment, especially the insulating granular particles. This is because they work well and are reliable [19].

Utilizing numerical methods to model the separation process plays a vital role in minimizing the need for extensive experimental trials, as it offers deep insights into the associated physical phenomena. Consequently, researchers have employed particle trajectory simulations to investigate how different parameters impact the efficiency and result of the separation process [2].

The **goal** of the work is to represent graphically the trajectories of two insulating charged polypropylene particles of different sizes (2 mm and 4 mm) in the multifunctional electrostatic separator powered by photovoltaic (PV) system use a multipoint electrodes as charging device employing numerical simulation and demonstrate its effectiveness and reliability for the study of particles trajectories by integrating PV panels as a power source for electrostatic separators according to the recommendations of the new energy system.

The use of PV panels ensures the required voltage to power the suggested electrostatic separator. During the separation process, a 2 mm and 4 mm insulating particles are charged as they pass through the charge zone by coronal discharge generated by the multipoint configuration with the same charge as the electrode. They then reach the separation zone, where they are separated in the presence of an intense electric field. This work aims to represent graphically the charged particles trajectories using numerical simulation, demonstrate their effectiveness and reliability for the study of particles trajectories and improve the efficiency of electrostatic separators.

Methods. Multifunctional electrostatic separator description. Figure 1,*a* shows a design of a multifunctional electrostatic separator with two flexible verticals electrodes, powered by PV system. This system powered the separator.

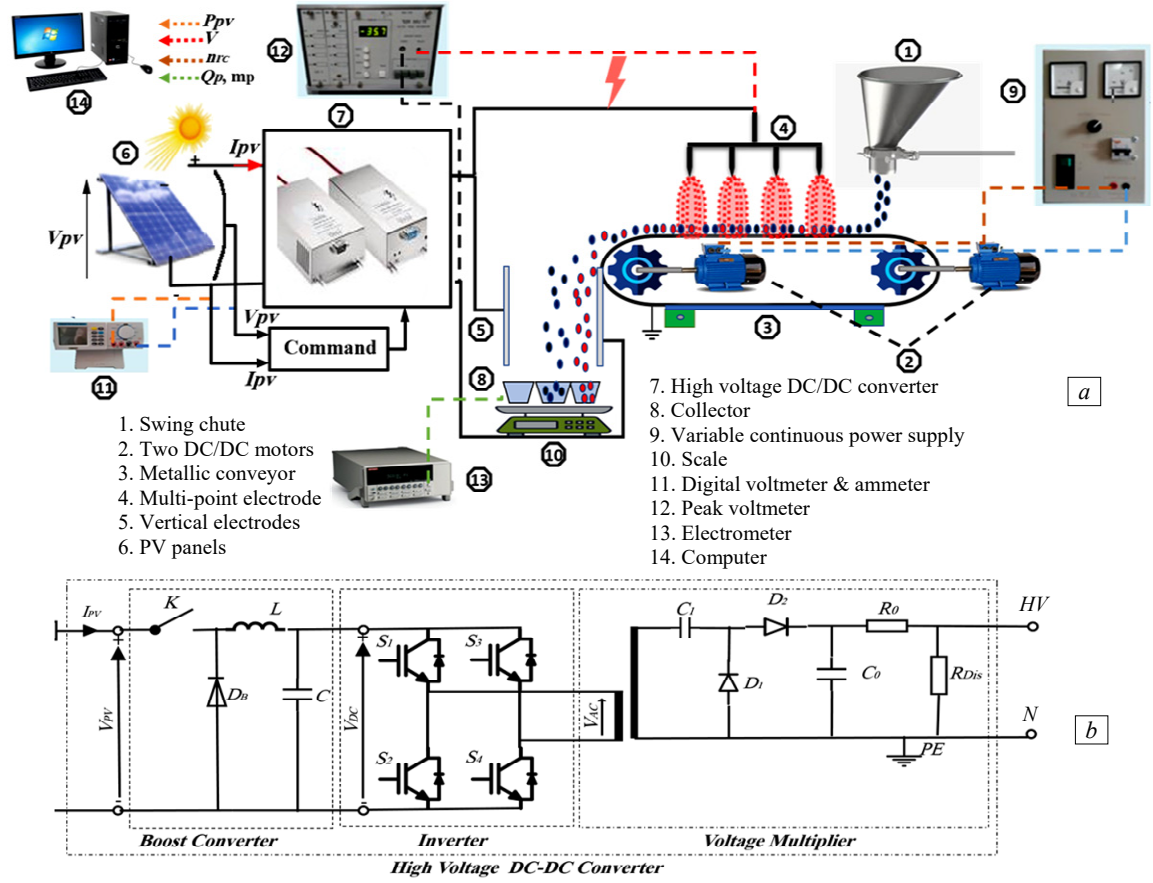

Fig. 1. *a* – multifunctional electrostatic separator with two flexible vertical electrodes powered by PV panels; *b* – basic electrical circuit that explains the conversion of the low-voltage primary source of direct voltage to high direct voltage for powered the separator

The design consists of a grounded metal belt conveyor, measuring 1000 mm in length and 100 mm in width. The conveyor belt is responsible for transporting the particles in the form of homogeneous spheres deposited on its surface to the electrical charging zone and the separation zone. This conveyor belt is driven by two DC or three-phase motors. These two motors are powered by an adjustable voltage source and rotated at an appropriate speed, where the charged particles fall into the electrostatic separation zone. A multi-point corona electrode in the form of needles perpendicular to the metal belt of the conveyor belt to generate corona discharges used to charge insulating particles. It consists of four points set 20 mm higher than the surface of the belt. Each point is 130 mm long and 2 mm in diameter, spaced 20 mm apart.

An electrostatic separation zone consists of two flexible vertical electrodes in the form of plates measuring 200 mm wide and 300 mm long, separated by a distance of 80 mm. The two electrodes can move back and forth between them.

The corona electrode and one of the vertical electrodes are connected to a 30 kV via a 500 V/30 kV high voltage DC/DC converter supplied by fourteen PV panels (Fig. 1,*b*). The voltages applied to the electrodes can vary from 20 kV to 30 kV for specific applications.

The multi-point electrode generates corona discharges that expose the insulating particles. They acquire electrical charges of the similar sign as the voltage applied to the corona electrode and fall into the electrostatic separation zone. When they freely fall into the separation zone, they are attracted to the electrode of opposite polarity and fall into the right part of the collector. However, the uncharged insulating particles, located in an intense electric field at the separation zone, fall into the middle part of the collector. The left part of the collector remains unchanged. Three collector boxes collect the separated insulating particles. The boxes are divided into two compartments and constituted in the form of a Faraday cage connected to an electrometer for measuring electrical charges, set on an electronic scale by measuring the mass of the separated particles.

You can record real-time information about how this electrostatic separator is working on a computer. The computer can record the power produced by the PV panels (P_{pv}), the voltages applied to the two active electrodes (V), the speed of the metal belt on the conveyor (n_{rc}), the number of charges on the particles (Q_p) and the masses of the particles (m_p).

Numerical modeling. This section involves the numerical modeling of the PV panels that power the electrostatic separator suggested, the electric field, the motion of the charged particles and their trajectories in the separation zone.

PV panel modeling. A PV panel, otherwise called a PV module, is generally made up of a set of elementary PV cells manufactured in the form of a thin layer of P-N junction semiconductor. These PV cells are connected in series and/or in parallel in order to obtain the required current, the required voltage, and the necessary power required to supply the load, due to the fact that each PV cell has a low nominal power. Figure 2 presents the model of the equivalent electrical circuit of a PV cell [21–23].

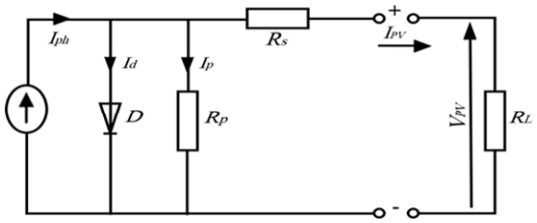

Fig. 2. The single-diode model represents the equivalent electrical circuit of a monocrystalline PV cell

The expression of the current generated by the single-diode PV cell is given as follows:

$$I_{ph} = I_d + I_p + I_{pv}; \quad (1)$$

$$I_{pv} = I_{ph} - I_d - I_p = \\ = I_{ph} - I_0 \cdot \left[\exp\left(\frac{q \cdot (V_{pv} + R_s \cdot I_{pv})}{n \cdot k_B \cdot T}\right) - 1 \right] - \frac{V_{pv} + R_s \cdot I_{pv}}{R_p}, \quad (2)$$

where I_{ph} is the photocurrent of the PV cell; I_d is the current at the diode junction; I_p is the current in the resistor R_p; I_{pv} is the output current of the PV cell; I_0 is the saturation current of the diode or the dark current; V_{pv} is the output voltage of the PV cell; R_s, R_p are the series and parallel resistances of the PV cell; n is the ideality coefficient of the cell; k_B is the Boltzmann constant; q is the electron charge; T is the temperature of the PV cell.

The following equation provides the mathematical model for the PV panel, assuming that all the cells are identical:

$$I_{pv} = N_p \cdot I_{ph} - \\ - N_p \cdot I_0 \cdot \left[\exp\left(\frac{q \cdot (N_s \cdot V_{pv} + (N_s/N_p) \cdot R_s \cdot I_{pv})}{n \cdot k_B \cdot T}\right) - 1 \right] - \quad (3) \\ - \frac{N_s \cdot V_{pv} + (N_s/N_p) \cdot R_s \cdot I_{pv}}{(N_s/N_p) \cdot R_p},$$

where N_s is the number of cells in series; N_p is the number of cells in parallel.

Electrical field modeling. This study uses a numerical model of the electric field to study the motion and trajectory of charged particles in electrostatic separators. The electric field is an important and essential factor for the electrostatic separation process. The electric field is responsible for the charge and the motion of the particles through the electrostatic force it generates. It is generated by applying a high voltage to the active electrode and the grounded electrode. To obtain the electric field strength $\boldsymbol{E}$, it must solve the Laplace equation or the Poisson equation, both of which are partial differential equations or use the COMSOL Multiphysics software, that uses the FEM [2, 24, 25] it can be expressed as follows:

$$\boldsymbol{E} = -\nabla V, \quad (4)$$

where $\boldsymbol{E}$ is the electric field intensity vector; V is the electric scalar potential. The boundary conditions are [24]:

- The potential on the active electrode is equal to the high applied voltage.
- The potential on the grounded electrode is zero.
- The electric field on the active electrode is equal to the onset field strength.

Modeling the motion of charged particles and their trajectories. While moving, particles that have been

charged by the corona discharge used in this study are affected by electrostatic force, gravitational force, and aerodynamic force. When they fall freely at the middle of the electrostatic separation zone, where there is a strong electric field, they are subject to all of these forces [26–28].

Gravitational force F_g. Any charged particle with a mass m_p experiences a gravitational force during free fall. The following relationship determines its value:

$$F_g = \begin{bmatrix} F_{g,x} \\ F_{g,y} \end{bmatrix} = \begin{bmatrix} 0 \\ -m_p \cdot g \end{bmatrix}, \quad (5)$$

where m_p is the mass of the charged particle, and g is the gravitational constant (g= 9.81 m/s).

Electrostatic force F_{el}. Any charged particle Q_p located in a region of intense electric field is subject to an electric force of attraction or repulsion. Coulomb's law expresses it this way:

$$F_{el} = \begin{bmatrix} F_{el,x} \\ F_{el,y} \end{bmatrix} = Q_p \cdot \begin{bmatrix} E_x(x,y) \\ E_y(x,y) \end{bmatrix}, \quad (6)$$

where Q_p is the charge of the charged particle, E_x, E_y are the horizontal and vertical components of the electric field vector, respectively.

Aerodynamic force F_{aero}. Any charged particle in the form of a homogeneous sphere of radius r_p experiences an aerodynamic force when it rubs against the air. The following formula gives the aerodynamic force:

$$F_{aero} = \begin{bmatrix} F_{aero,x} \\ F_{aero,y} \end{bmatrix} = \frac{1}{2} \cdot C_f \cdot \rho \cdot \pi \cdot r_p^{\,2} \cdot v \begin{bmatrix} v_x \\ v_y \end{bmatrix}, \quad (7)$$

where C_f = 0.5 is the coefficient of friction; ρ is the density of air; r_p is the radius of the charged particle; v_x, v_y are the components of the vector of the relative velocity of the particle.

Gravitational, electrostatic and aerodynamic forces act on the motion of charged particles, according to Newton's second law. It is defined by the following relationship [29–31]:

$$m_p \cdot a_n = \sum F = F_g + F_{el} + F_{aero}, \quad (8)$$

where a_n is the particle acceleration.

For represent graphically the trajectory of charged particles, we based on the Euler-Cromer method to solve the equation of motion numerically. This method is given by the following relation [28]:

$$v_{n+1} = v_n + a_n \cdot \Delta t; \quad (9)$$

$$p_{n+1} = p_n + v_{n+1} \cdot \Delta t, \quad (10)$$

where v is the velocity; p is the position; Δt is time step.

Results and discussion. In this paper we present the current-voltage (I–V) and power-voltage (P–V) characteristics of 14 PV panels by varying the solar irradiation using the PV module characteristics (Table 1), the evolution of the electric field in the electrical charging zone and the separation zone (Fig. 3) through the COMSOL Multiphysics program for two configurations (Table 2) and the graphical representation of the trajectories of two polypropylene insulating particles of 2 mm and 4 mm sizes in the separation zone through the Euler-Cromer method was programmed in MATLAB by varying the value of the voltage applied to the active electrodes and the inter-electrode distance and by injecting the intensity of the electric field previously obtained. The particle sizes for which the Euler-Cromer method is most effective range from 1 mm to 5 mm [2, 28].

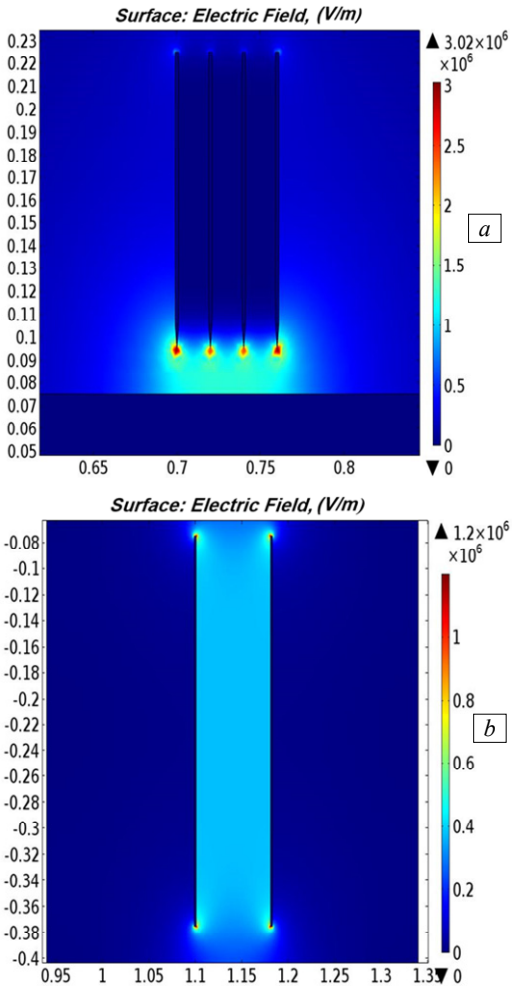

Fig. 3. The distribution of electric field:
a – the electric charging zone; *b* – the electrostatic separation zone

Table 1

PV characteristics of an ETSolar PV module

Reference	ET-M572185
Maximum power P_{max}, W	185
Open circuit voltage V_{oc}, V	44.6
Short circuit current I_{sc}, A	5.8
Rated voltage V_{mpp}, V	36.3
Rated current I_{mpp}, A	5.09
Cell per module	72

Table 2

Two configurations of the inter-electrode distance

Configurations	D_1, mm	D_2, mm	D_3, mm
Multipoint-conveyor	60	40	20
Verticals electrodes	80	95	110

PV characteristics of the ETSolar PV panels. Figure 4 shows I–V and P–V characteristics of 14 ET-M572185 panels. These panels are linked in series to power the multifunctional electrostatic separator with two flexible verticals electrodes with a voltage of 30 kV via a high-voltage converter DC/DC of 500 V / 30 kV. The measurements were carried out at a temperature of 25 °C and 3 different solar radiation values (800 W/m^2, 900 W/m^2, 1000 W/m^2). Each of these solar radiation values corresponds to a maximum electrical power that the 14 panels could provide.

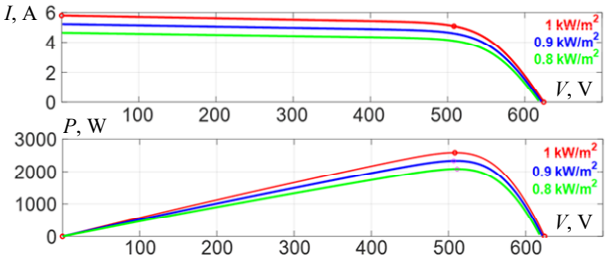

Fig. 4. *I–V* and *P–V* characteristics of 14 modules of type ET-M572185 at 25 °C

Electric field variation. Electrical charging zone. Figure 5 depicts the electric field variation at the conveyor generated by 4 points as a function of their positions *p*, which represents the electrical charging zone of insulating particles for an applied voltage of 30 kV and an inter-electrode distance of 20 mm. The multipoint-conveyor configuration allows the insulating particles to cross the region of the intense electric field produced by each point and acquire electric charges of the same sign as those of the corona electrode.

Figures 6, 7 show the electric field variation at the conveyor for 3 different applied voltages (20 kV, 25 kV, 30 kV) and 3 different inter-electrode distances for a multipoint-conveyor configuration shown in Table 2.

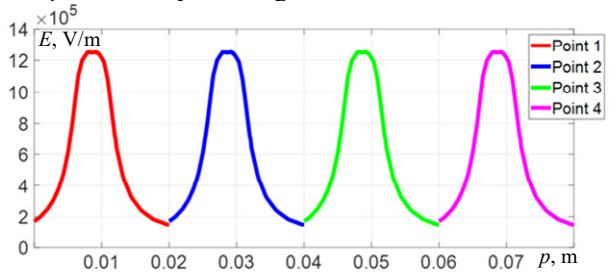

Fig. 5. Electric field variation at the conveyor

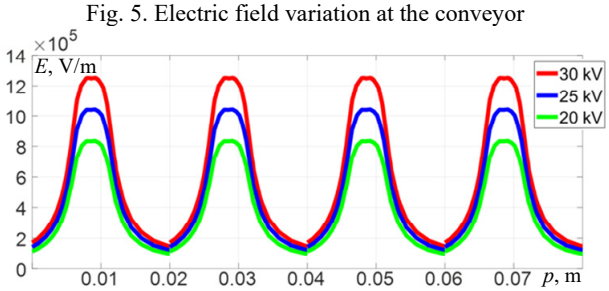

Fig. 6. Electric field variation at the conveyor for different applied voltages

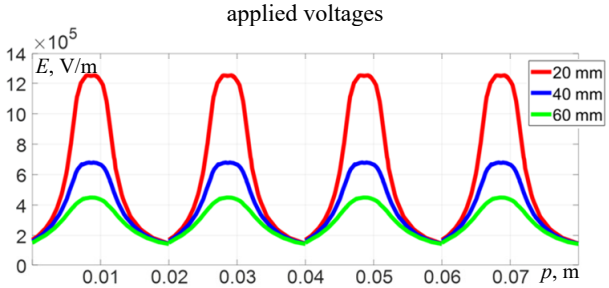

Fig. 7. Electric field variation at the conveyor for different distances

Electrostatic separation zone. Figures 8, 9 show the electric field variation generated in the separation zone. These results are for 3 values of the applied voltage of 20 kV, 25 kV and 30 kV and 3 values of the inter-electrode distance – 80 mm, 95 mm and 110 mm. The curves show that the electric field is uniform in this region. It is strong and intense, with a value of $3.75 \cdot 10^5$ V/m for a 30 kV voltage and an 80 mm distance between the electrodes. This investigation demonstrates the importance of the electric field process in electrostatic separators. That is electrostatic separation requires an intense electric field of the order of 10^6 V/m.

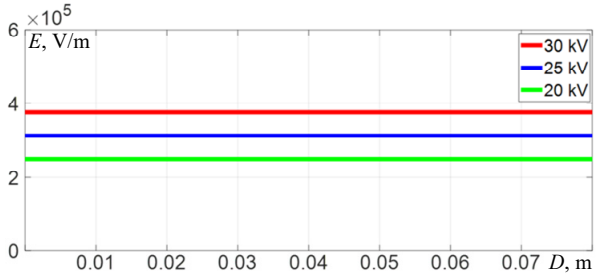

Fig. 8. Electric field variation at the ground for different applied voltages

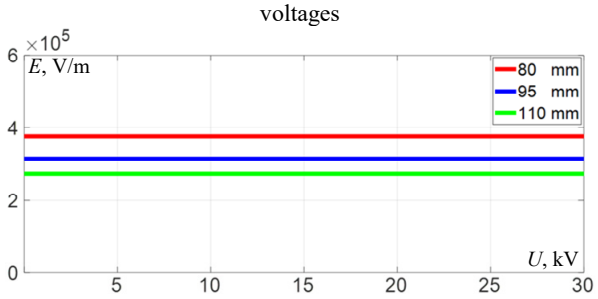

Fig. 9. Electric field variation at the ground for different distances

Trajectories of the charged particles in the electrostatic separation zone. We illustrate in Fig. 10–13 the trajectories of 2 mm and 4 mm polypropylene particle in the separation zone for three different values of the voltage applied to the active electrode (20 kV, 25 kV and 30 kV) and three different distances between the electrodes of 80 mm, 95 mm and 110 mm. These trajectories were obtained numerically.

For the case of a variation of the applied voltage and the distance, we can observe that the charged particle of size 2 mm is attracted with a strong acceleration by the opposite electrode without colliding with it. Moreover, the other electrode repels it when its sign matches. Indeed, the electrostatic force is dominant compared to the gravitational force due to the lightness and small diameter of the particle. Finally, the charged particle gathers in the left compartment of the collector box.

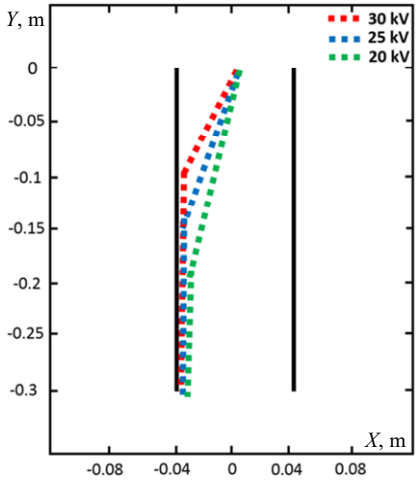

Fig. 10. 2 mm polypropylene particle trajectories for different voltages applied at an inter-electrode distance of 80 mm

In the case of a charged particle of size 4 mm, we can note that there is a ratio between the gravitational

force and the electrostatic force. As expected, the gravitational force is dominant compared to the electrostatic force. The large-diameter charged particle makes a slow acceleration due to the effect of gravitational force. The deflection of the charged particle increases proportionally to the increase in the applied voltage while keeping the same tangent, and it collects in the right compartment of the collector box.

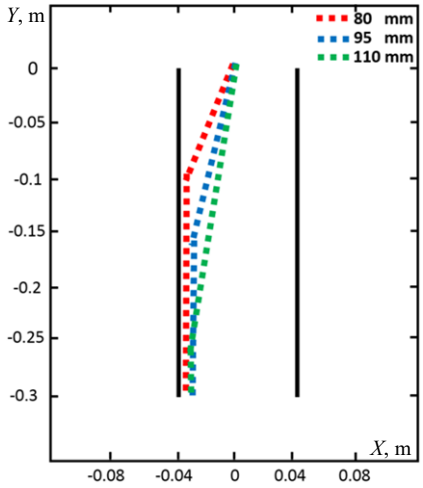

Fig. 11. 2 mm polypropylene particle trajectories for different distances at an applied voltage of 30 kV

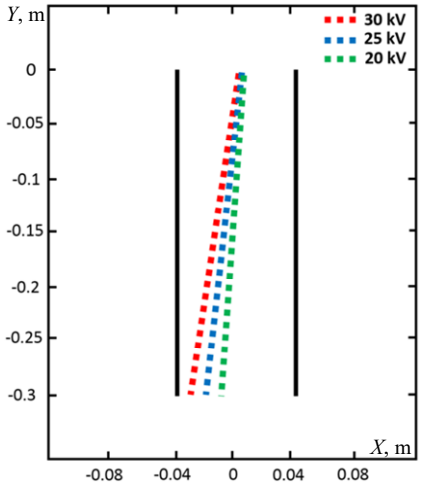

Fig. 12. 4 mm polypropylene particle trajectories for different voltages applied at a distance of 80 mm

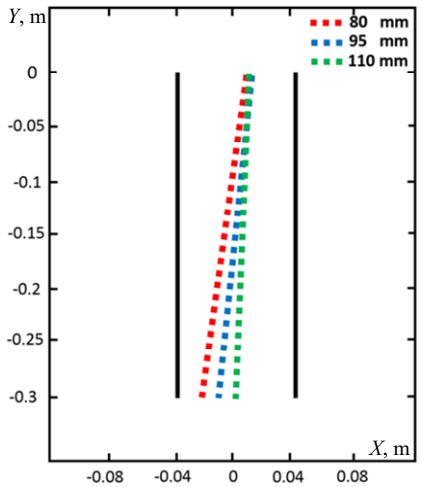

Fig. 13. 4 mm polypropylene particle trajectories for different distances at an applied voltage of 30 kV

Figure 14 shows the trajectories of two polypropylene particles of 2 mm and 4 mm sizes when a voltage of 30 kV is applied and there is an inter-electrode distance of 80 mm.

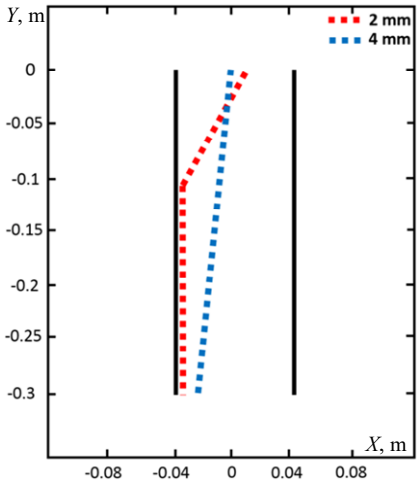

Fig. 14. 2 mm and 4 mm polypropylene particle trajectories at 30 kV and 80 mm

Conclusions. A design of the multifunctional electrostatic separator and the simulation results obtained in this article allow us to formulate the following conclusions.

The integration of PV system as a power source for electrostatic separators, and give it high priority according the recommendation of the new energy system due to its numerous advantages and effective contribution to sustainable development.

The multi-point configuration used in this work has a high efficiency for charging the insulating particles.

The numerical model based on the Euler-Cromer method that based on the calculation of the electric field intensity, which is done by the COMSOL Multiphysics software, and programmed in MATLAB software, is an effective and validated tool for the study of the particles trajectories. The numerical simulation has provided a profound comprehension of various phenomena that occur in the electrostatic separation zone. It is also considered a tool to validate experimental results.

Directions for further research may be the following: To conduct this work experimentally in the future and study the trajectories of conductive and nonconductive particles in the proposed electrostatic separator.

Conflict of interest. The authors declare that they have no conflicts of interest.

REFERENCES

1. Senathirajah K., Attwood S., Bhagwat G., Carbery M., Wilson S., Palanisami T. Estimation of the mass of microplastics ingested – A pivotal first step towards human health risk assessment. *Journal of Hazardous Materials*, 2021, vol. 404, art. no. 124004. doi: https://doi.org/10.1016/j.jhazmat.2020.124004.

2. Maammar M., Achouri I.-E., Zeghloul T., Medles K., Aksa W., Dascalescu L. Numerical Simulation and Experimental Observation of Charged Particles Trajectories in Roll-Type Electrostatic Separators. *IEEE Transactions on Industry Applications*, 2021, vol. 57, no. 6, pp. 6504-6511. doi: https://doi.org/10.1109/TIA.2021.3103485.

3. Baldé C.P., Kuehr R., Yamamoto T. et al. Global Report on Waste Electrical and Electronic Equipment. *The Global E-waste Monitor*, 2024. 148 p. Available at: https://ewastemonitor.info/wp-content/uploads/2024/03/GEM_2024_18-03_web_page_per_page_web.pdf (Accessed 07 May 2025).

4. Guettaf N., Anane Z., El Islem Guettaf S., Hassaine F., Nouri H. Study of the different parameter corona discharge in point-plane

Electrostatic Separator. *2022 19th International Multi-Conference on Systems, Signals & Devices (SSD)*, 2022, pp. 1831-1835. doi: https://doi.org/10.1109/SSD54932.2022.9955502.
5. Mekhalef Benhafssa A., Medles K., Boukhoulda M.F., Tilmatine A., Messal S., Dascalescu L. Study of a Tribo-Aero-Electrostatic Separator for Mixtures of Micronized Insulating Materials. *IEEE Transactions on Industry Applications*, 2015, vol. 51, no. 5, pp. 4166-4172. doi: https://doi.org/10.1109/TIA.2015.2434794.
6. He J., Tang H., Guo C., Zhu L., Huang S., Yang B. Synergist enhancement of effective desilication of graphite ore by rotary triboelectric separation and surface modification. *Powder Technology*, 2024, vol. 444, art. no. 119965. doi: https://doi.org/10.1016/j.powtec.2024.119965.
7. He J., Huang S., Chen H., Zhu L., Guo C., He X., Yang B. Recent advances in the intensification of triboelectric separation and its application in resource recovery: A review. *Chemical Engineering and Processing - Process Intensification*, 2023, vol. 185, art. no. 109308. doi: https://doi.org/10.1016/j.cep.2023.109308.
8. Pan X., Wong C.W.Y., Li C. Circular economy practices in the waste electrical and electronic equipment (WEEE) industry: A systematic review and future research agendas. *Journal of Cleaner Production*, 2022, vol. 365, art. no. 132671. doi: https://doi.org/10.1016/j.jclepro.2022.132671.
9. Bedeković G., Trbović R. Electrostatic separation of aluminium from residue of electric cables recycling process. *Waste Management*, 2020, vol. 108, pp. 21-27. doi: https://doi.org/10.1016/j.wasman.2020.04.033.
10. Perdana T., Kusnandar K., Perdana H.H., Hermiatin F.R. Circular supply chain governance for sustainable fresh agricultural products: Minimizing food loss and utilizing agricultural waste. *Sustainable Production and Consumption*, 2023, vol. 41, pp. 391-403. doi: https://doi.org/10.1016/j.spc.2023.09.001.
11. Radebe N., Chipangamate N. Mining industry risks, and future critical minerals and metals supply chain resilience in emerging markets. *Resources Policy*, 2024, vol. 91, art. no. 104887. doi: https://doi.org/10.1016/j.resourpol.2024.104887.
12. Sun B., Li B., Ma S., Zhu M., Dong C., Xiang M., Cheng H., Yu Y. The recycling potential of unregulated waste electrical and electronic equipment in China: Generation, economic value, and cost-benefit analysis. *Journal of Cleaner Production*, 2023, vol. 402, art. no. 136702. doi: https://doi.org/10.1016/j.jclepro.2023.136702.
13. Shahabuddin M., Uddin M.N., Chowdhury J.I., Ahmed S.F., Uddin M.N., Mofijur M., Uddin M.A. A review of the recent development, challenges, and opportunities of electronic waste (e-waste). *International Journal of Environmental Science and Technology*, 2023, vol. 20, no. 4, pp. 4513-4520. doi: https://doi.org/10.1007/s13762-022-04274-w.
14. Gao Y., Huang X., Xia D., Lyu C. Research on the recycling decision of WEEE in rural China under dual supervision. *Scientific Reports*, 2024, vol. 14, no. 1, art. no. 23875. doi: https://doi.org/10.1038/s41598-024-74158-1.
15. Catinean A., Dascalescu L., Lungu M., Dumitran L.M., Samuila A. Improving the recovery of copper from electric cable waste derived from automotive industry by corona-electrostatic separation. *Particulate Science and Technology*, 2021, vol. 39, no. 4, pp. 449-456. doi: https://doi.org/10.1080/02726351.2020.1756545.
16. Zeghloul T., Touhami S., Richard G., Miloudi M., Dahou O., Dascalescu L. Optimal Operation of a Plate-Type Corona-Electrostatic Separator for the Recovery of Metals and Plastics from Granular Wastes. *IEEE Transactions on Industry Applications*, 2016, vol. 52, no. 3, pp. 2506-2512. doi: https://doi.org/10.1109/TIA.2016.2533482.
17. Touhami S., Aksa W., Medles K., Tilmatine A., Dascalescu L. Numerical Simulation of the Trajectories of Insulating Particles in a Tribo-Aero-Electrostatic Separator. *IEEE Transactions on Industry Applications*, 2015, vol. 51, no. 5, pp. 4151-4158. doi: https://doi.org/10.1109/TIA.2015.2427276.
18. Tilmatine A., Benabboun A., Brahmi Y., Bendaoud A., Miloudi M., Dascalescu L. Experimental Investigation of a New Triboelectrostatic Separation Process for Mixed Fine Granular Plastics. *IEEE Transactions on Industry Applications*, 2014, vol. 50, no. 6, pp. 4245-4250. doi: https://doi.org/10.1109/TIA.2014.2319584.
19. Kimi I.E., Benhammou A., Touhami S., Rezoug M. Numerical modelling and experimental validation of an Enhanced multi-force model of free-fall electrostatic separators. *Particulate Science and Technology*, 2025, vol. 43, no. 1, pp. 52-64. doi: https://doi.org/10.1080/02726351.2024.2417363.
20. Székely L., Kiss I., Donghyeok G. Investigation of the separation of conductive and insulating objects on a laboratory made electrostatic separator. *Journal of Physics: Conference Series*, 2024, vol. 2702, no. 1, art. no. 012010. doi: https://doi.org/10.1088/1742-6596/2702/1/012010.
21. Latreche K., Taleb R., Bentaallah A., Toubal Maamar A.E., Helaimi M., Chabni F. Design and experimental implementation of voltage control scheme using the coefficient diagram method based PID controller for two-level boost converter with photovoltaic system. *Electrical Engineering & Electromechanics*, 2024, no. 1, pp. 3-9. doi: https://doi.org/10.20998/2074-272X.2024.1.01.
22. Bounechba H., Boussaid A., Bouzid A. Experimental validation of fuzzy logic controller based on voltage perturbation algorithm in battery storage photovoltaic system. *Electrical Engineering & Electromechanics*, 2024, no. 5, pp. 20-27. doi: https://doi.org/10.20998/2074-272X.2024.5.03.
23. Zorig A., Babes B., Hamouda N., Mouassa S. Improving the efficiency of a non-ideal grid coupled to a photovoltaic system with a shunt active power filter using a self-tuning filter and a predictive current controller. *Electrical Engineering & Electromechanics*, 2024, no. 6, pp. 33-43. doi: https://doi.org/10.20998/2074-272X.2024.6.05.
24. Guettaf N., Said H.A., Aissou M., Zegloul T., Nouri H. Modeling a Corona Discharge Separation of Fine Particles for Different Materials Used in Electrical Engineering. *Advanced Engineering Forum*, 2025, vol. 54, pp. 77-90. doi: https://doi.org/10.4028/p-U8GCnx.
25. Grechko O.M. Influence of the poles shape of DC electromagnetic actuator on its thrust characteristic. *Technical Electrodynamics*, 2024, no. 1, pp. 38-45. doi: https://doi.org/10.15407/techned2024.01.038.
26. Ireland P.M. Modelling dense particle streams during free-fall electrostatic separation. *Powder Technology*, 2024, vol. 434, art. no. 119290. doi: https://doi.org/10.1016/j.powtec.2023.119290.
27. Qin Y., Gao K., Li J., Xu Z. Particle trajectory model for tribo-electrostatic separating mixed granular plastics. *Cleaner Engineering and Technology*, 2021, vol. 4, art. no. 100219. doi: https://doi.org/10.1016/j.clet.2021.100219.
28. Maammar M., Touhami S., Rezoug M., Daioui K., Dascalescu L., Medles K. Experimental study and numerical simulation of particles trajectories in a flexible-electrode-type electrostatic separator. *Journal of Physics: Conference Series*, 2024, vol. 2702, no. 1, art. no. 012018. doi: https://doi.org/10.1088/1742-6596/2702/1/012018.
29. Xu Z., Li J., Lu H., Wu J. Dynamics of conductive and nonconductive particles under high-voltage electrostatic coupling fields. *Science in China Series E: Technological Sciences*, 2009, vol. 52, no. 8, pp. 2359-2366. doi: https://doi.org/10.1007/s11431-008-0198-2.
30. Labair H., Touhami S., Tilmatine A., Hadjeri S., Medles K., Dascalescu L. Study of charged particles trajectories in free-fall electrostatic separators. *Journal of Electrostatics*, 2017, vol. 88, pp. 10-14. doi: https://doi.org/10.1016/j.elstat.2017.01.010.
31. Touhami S., Aksa W., Maammar M., Zeghloul T., Medles K., Dascalescu L. Numerical simulation of the behavior of insulating particles in a free fall tribo-electrostatic separator with four vertical cylindrical electrodes. *Journal of Electrostatics*, 2019, vol. 97, pp. 8-14. doi: https://doi.org/10.1016/j.elstat.2018.11.004.

Received 25.07.2025
Accepted 12.09.2025
Published 02.01.2026

N. Guettaf[1]*, PhD,*
S.E.I. Guettaf[2]*, PhD,*
T. Zeghloul[3]*, Professor,*
H. Nouri[1]*, Professor,*
[1] Department of Electrical Engineering, LAS Laboratory, Setif 1 University - Ferhat Abbas, Setif, 19000, Algeria, e-mail: nacereddine.guettaf94@gmail.com (Corresponding Author)
[2] Department of Electrical Engineering, QUERE Laboratory, Setif 1 University - Ferhat Abbas, Setif, 19000, Algeria.
[3] IUT Angoulême, Pprime Institute-ENSMA, Poitiers University, Angoulême, 16000, France.

How to cite this article:
Guettaf N., Guettaf S.E.I., Zeghloul T., Nouri H. Numerical study of particles trajectories in a multifunctional electrostatic separator powered by photovoltaic system. *Electrical Engineering & Electromechanics*, 2026, no. 1, pp. 69-75. doi: https://doi.org/10.20998/2074-272X.2026.1.09